



Open pit mine planning considering geomechanical fundamentals

Andrés Parra, Nelson Morales, Javier Vallejos & Phu Minh Vuong Nguyen

To cite this article: Andrés Parra, Nelson Morales, Javier Vallejos & Phu Minh Vuong Nguyen (2018) Open pit mine planning considering geomechanical fundamentals, International Journal of Mining, Reclamation and Environment, 32:4, 221-238, DOI: [10.1080/17480930.2017.1278579](https://doi.org/10.1080/17480930.2017.1278579)

To link to this article: <https://doi.org/10.1080/17480930.2017.1278579>



Published online: 13 Jan 2017.



Submit your article to this journal [↗](#)



Article views: 165



View related articles [↗](#)



View Crossmark data [↗](#)



Open pit mine planning considering geomechanical fundamentals

Andrés Parra^{a,b}, Nelson Morales^{a,b}, Javier Vallejos^b and Phu Minh Vuong Nguyen^{a,b} 

^aDelphos Mine Planning Laboratory, University of Chile, Santiago, Chile; ^bMining Engineering Department & Advanced Mining Technology Center, University of Chile, Santiago, Chile

ABSTRACT

The objective of this study is to integrate the admissible factor of safety (FoS) into the mine planning. The analysis showed, as expected, that a lower net present value (NPV) is obtained with the increase in the admissible FoS. Most importantly, it demonstrated that the FoS of the slopes of the adjacent phases, which are not part of the final pit, are considerably greater than the admissible FoS. Therefore, the NPV of an open pit mine project can be increased by steepening the slopes of adjacent phases that are not part of the final pit walls.

ARTICLE HISTORY

Received 4 October 2016
Accepted 1 January 2017

KEYWORDS

Open pit mine planning;
slope design; slope stability;
factor of safety; open pit
mine designs

1. Introduction

Over the last decades, the depth reached by some open pits has grown considerably (Figure 1). With the deepening of the pits, particular focus has been placed on slope angles, because of their influence on the economic and safety of the mine: increasing the slope angle leads to less waste removal but it may also lead to slope's instabilities and may result in considerable losses of material, equipment and/or personnel [1,2].

An example of the dangers of slope instability is the slope failure incident at Bingham Canyon copper mine in Utah, United States, during which 165 million tonnes of rocks plummeted over more than a half mile to the bottom of the pit (Figure 2) and the mine's production was cut in half [3]. This example clearly shows the importance of safety to ensure a continuous operation throughout the life of the mine [4].

Several factors must be taken into account during the mine planning process to fulfil the main goal of the open pit mine planning to maximise the value of the business according to the strategic objectives of the mining company. These factors include the economic parameters, such as, costs and commodity prices that allow the mine valuation of all ores present and the extraction costs of ores and waste materials. Furthermore, the geometrical characteristics, used to design and optimise the pit, are highly relevant to the project's economics and safety, as they are associated with acceptable design criteria, which determine the stability of the open pit's walls. Among these characteristics are bench face angle, bench height, berm width, inter-ramp angle, overall angle, overall height and ramp width.

The determination of the geometrical components of a slope is based on acceptable design criteria, typically expressed in terms of the Factor of Safety (FoS), which is the relationship between resisting and driving forces of the rock mass [5], and in terms of the operational requirements, such as, loading equipment, which generally determines the bench height.

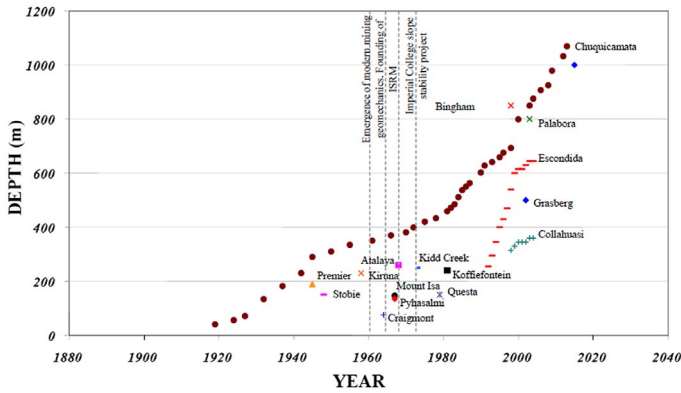


Figure 1. Historical evolution of open pit mines' depth [4].



Figure 2. Landslide at Bingham Canyon copper mine in Utah, United States [3].

Slope stability is significantly influenced by the slope angles, the parameters of the rock mass strength, the geological structure of the rock mass, the geometry of the pit slope, the conditions of stress, groundwater, discontinuities, blasting and seismic events or conditions of weathering and climate. In addition, time is an important factor influencing the slope stability as many specific factors change over time, the groundwater level changes with seasons, the excavation and seismic phenomena are irregular, weathering may cause changes in the chemical and structural characteristics of the rock mass and continuous small-scale activities change the stress and load on the slope. Understanding of all these factors would assist in better design and prevention of slope instability.

The influence of slope angles on the pit value and design and its dependency on the depth of the pit is well known [16].

In this paper, the aim is to investigate closer the relationship and the integration between geomechanics and mine planning. Therefore, the impact of the FoS on mine planning is studied. Specifically, the variation in the final pit shell, mine designs, mine scheduling and mine plans' economical evaluation are studied when changing the admissible FoS of the slopes at an open pit mine.

This paper is organised as follows. Sections 2–4 provide a review of the Hoek–Brown failure criterion, the methods of slope stability analysis and the aspects of open pit mine planning that are relevant to this work. Section 5 presents the case study and Section 6 presents and discusses the results of the application. Finally, Section 7 contains the conclusions of this research.

Table 1. General form of the Hoek–Brown failure criteria.

The generalised Hoek–Brown criterion	$\sigma'_1 = \sigma'_3 + \sigma_c \left(m_b \frac{\sigma'_3}{\sigma_c} + s \right)^a$
The relationship between m_b/m_i , s and the GSI	$m_b = m_i e^{\frac{\text{GSI}-100}{28}}$
For GSI > 25 (rock masses of good to reasonable quality)	$s = e^{\frac{\text{GSI}-100}{9}}; a = 0.5$
For GSI < 25 (rock masses of very poor quality)	$s = 0; a = 0.65 - \frac{\text{GSI}}{200}$

2. Rock mass strength failure criteria

Commencing with the first failure criterion proposed by Coulomb at the end of the eighteenth century, a number of empirical studies related to the strength of intact rock have been published and the empirical failure equations have been proposed based on laboratory tests of intact rock specimens [6]. Some of the equations have been developed as rock mass failure criteria, with suitable adjustments related to the rock classification indexes, such as, rock mass rating (RMR), geological strength index (GSI) classification, and Hoek and Brown criterion [6]. The failure criteria for rock masses are based on large-scale and laboratory testing, experience and/or empirical analysis.

The most known and most used of these criteria is the Hoek–Brown failure criterion, which has been updated several times [7–13]. The original Hoek–Brown failure criterion was developed for both intact rock and rock mass in 1980. The peak triaxial strength of a wide range of rock materials could be reasonably represented by Equation (1):

$$\sigma_1 = \sigma_3 + \sqrt{m\sigma_3\sigma_{ci} + s\sigma_{ci}^2} \quad (1)$$

where σ_1 is the major principal stress, σ_3 is the minor principal stress, σ_{ci} is the uniaxial compressive strength of the intact rock mass, m and s are constants dependent on the properties of the rock and on the extent to which the rock has been broken before being subjected to the stresses σ_1 and σ_3 .

The modified version of the Hoek–Brown criterion for jointed rock masses can be written in the following form [14]:

$$\sigma'_1 = \sigma'_3 + \sigma_c \left(m_b \frac{\sigma'_3}{\sigma_c} \right)^a \quad (2)$$

where m_b and a are constants for the broken rock.

A general form of the Hoek–Brown failure criterion (Table 1) [10] incorporates both the original and the modified criteria for fair to very poor quality rock masses and which introduces a new index called the GSI (Figure 3).

In 2002, the modifications of the m_b , s and a were introduced according to Equations (3)–(5):

$$m_b = m_i \exp\left(\frac{\text{GSI} - 100}{28 - 14D}\right) \quad (3)$$

$$s = \exp\left(\frac{\text{GSI} - 100}{9 - 3D}\right) \quad (4)$$

$$a = \frac{1}{2} + \frac{1}{6} \left(e^{-\text{GSI}/15} - e^{-20/3} \right) \quad (5)$$

where D is a factor dependent on the degree of disturbance of the rock mass (between 0 and 1).

3. Methods of slope stability analysis

The methods used for the slope stability in this chapter are divided into three types: empirical, limit equilibrium and numerical.







		SURFACE CONDITIONS				
		VERY GOOD	GOOD	FAIR	POOR	VERY POOR
STRUCTURE		DECREASING SURFACE QUALITY →				
	INTACT OR MASSIVE - intact rock specimens or massive in situ rock with few widely spaced discontinuities	90			N/A	N/A
	BLOCKY - well interlocked undisturbed rock mass consisting of cubical blocks formed by three intersecting discontinuity sets	80	70			
	VERY BLOCKY- interlocked, partially disturbed mass with multi-faceted angular blocks formed by 4 or more joint sets		60	50		
	BLOCKY/DISTURBED/SEAMY - folded with angular blocks formed by many intersecting discontinuity sets. Persistence of bedding planes or schistosity			40	30	
	DISINTEGRATED - poorly interlocked, heavily broken rock mass with mixture of angular and rounded rock pieces				20	
	LAMINATED/SHEARED - Lack of blockiness due to close spacing of weak schistosity or shear planes	N/A	N/A			10

Figure 3. Estimation of GSI [15].

3.1. Empirical methods

Empirical methods for slope stability analysis are based on the knowledge of mine personnel about slope behaviour acquired at various mine sites around the world. This knowledge was gathered to create a database, which was used by Hoek and Bray [16] and, subsequently, by Sjöberg [1] to determine the relation between the slope height and the slope angle based on the steepest and highest slopes at specific open pit mines and to indicate the stable and unstable slopes (Figures 4 and 5).

However, these approaches did not recognise the differences in the failure mechanism, which controls the rock mass. Rock mass classification was applied to slope stability design charts by Bieniawski [17–19] using RMR and by Laubscher [20] using mining rock mass rating (MRMR). One of the best known and most widely used charts for determining slope stability was published by Haines and Terbrugge [21], which is based on the MRMR scheme (Figure 6).

The limitations of using design charts are related to their experimental and semi-quantitative nature. However, they allow the preliminary estimation of slope characteristics, especially, at the conceptual and pre-feasibility stages of a project development.

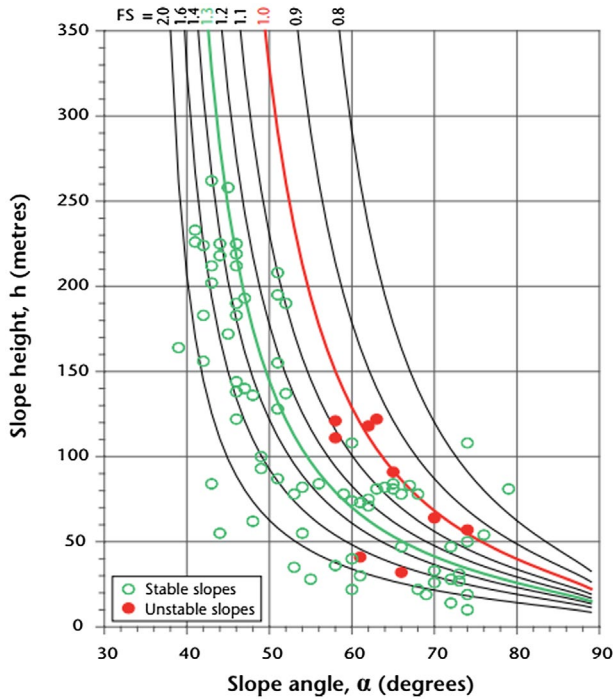


Figure 4. Relation of slope height vs. slope angle [16].

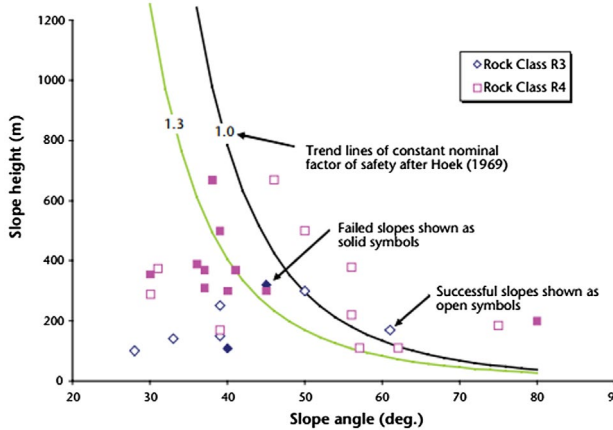


Figure 5. Rock slope stability designated by rock strength [1].

3.2. Limit equilibrium methods

The limit equilibrium analysis determines the slope safety factors based on a set of simplifying mechanical assumptions. In Limit equilibrium methods (LEM), measure of slope stability is the FoS, which is defined as a ratio between the sum of the forces acting to induce sliding of parts of the slope (driving forces) and the sum of the forces available to resist failure (resisting forces) (Equation (6)):

$$FoS = \frac{\sum (\text{Resisting Forces})}{\sum (\text{Driving Forces})} \tag{6}$$

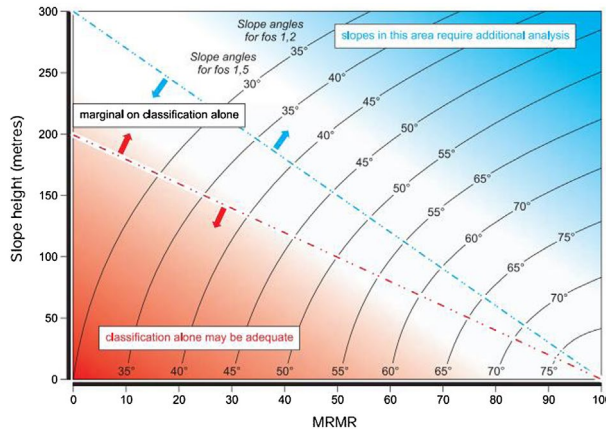


Figure 6. Chart for determining slope angle and slope height [21].

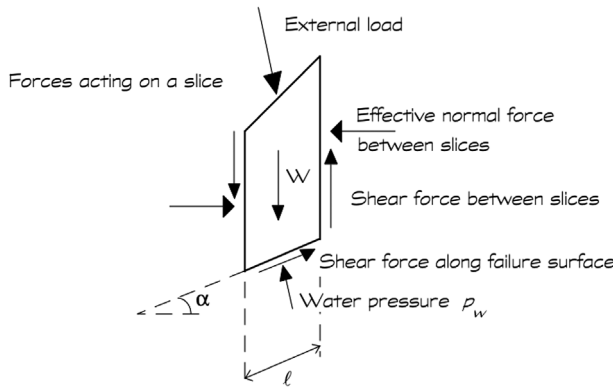


Figure 7. Forces acting on an individual slice in the Method of Slices [1].

The FoS can also be formulated as a ratio between the tangent stress related to the shear strength of rock mass and shear stress induced weight and other factors influencing the rock mass behaviour:

$$FoS = \frac{\tau_r}{\tau_s} = \frac{c + \sigma tg\varphi}{\tau_s} \tag{7}$$

where τ_r is maximum shear resistance estimated by Mohr–Coulomb Failure Criterion, τ_s is shear stress, c is cohesion, σ is normal stress, φ is friction angle.

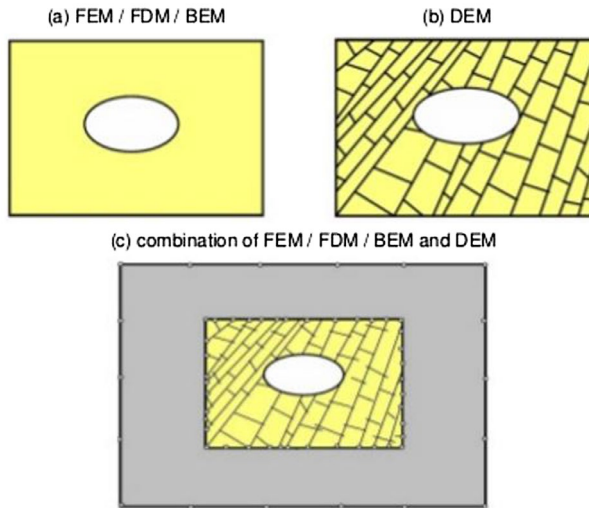
In LEM, the ore body is divided into slices above the candidate surface often assumed to be circular [22]. The forces acting on individual slice are shown in Figure 7. The associated equations and unknowns are shown in Table 2. Additional details of these methods can be found in a number of different literature sources [1,23,24].

3.3. Numerical methods

Rapid advances in computer science have increased the use of numerical methods in geoenvironmental analysis to evaluate rock mass behaviour, geological models, failure mechanisms and slope designs options. Moreover, these methods can model many of the complex conditions found in rock slopes, such as, non-linear stress–strain behaviour, anisotropy and changes in geometry. Generally, there are

Table 2. Equations and unknowns associated with the Method of Slices.

Equations	Condition	Unknowns	Variable
n	Moment equilibrium for slice ($\sum M = 0$)	1	Factor of safety, FoS
$2n$	Horizontal and vertical equilibrium for slice ($\sum F_h$ & $\sum F_v = 0$)	n	Normal force, N
n	Mohr–Coulomb equation	n	Position of N on sliding plane
$4n$	Total number of equations	n	Shear force, T
		$n - 1$	Horizontal interslice forces, E_i and E_{i+1}
		$n - 1$	Vertical interslice forces, X_i and X_{i+1}
		$n - 1$	Line of thrust, position of E_i and E_{i+1}
		$6n - 2$	Total number of unknowns

**Figure 8.** Numerical approaches to model rock engineering issues [25].

three possible approaches to model any individual rock-engineering problem: continuum, discontinuum and hybrid (Figure 8).

Continuum models are based on the assumption that the rock mass behaves as a continuum medium, i.e. it cannot be broken into pieces. Continuum codes, widely used for slope design, include finite element codes: PHASE² [26], ABAQUS and finite difference codes: FLAC 2D and FLAC 3D [27].

Discontinuum models imply that the rock mass behaves as a discontinued media consisting of a finite number of interacting bodies (faults, joints, blocks). Two widely used discontinuum codes for slope stability studies are UDEC and 3DEC [27].

Hybrid approaches attempt to maximise the advantages of continuum and discontinuum methods by combining them into one model, which represents the near field of object investigated with discontinuum elements and the far field using continuum material, therefore, improving computational efficiency. The codes of hybrid approaches are ELFEN [28], PFC2D and PFC3D [27].

These numerical methods are most useful for comparing the results with the observation, monitoring and measurements. However, the possibility of widespread application of numerical methods is limited mainly due to poor knowledge of the input parameters, such as, strength and deformation. In addition, a significant obstacle to the utilisation of numerical modelling is insufficient verification against real conditions.

From the reviewed literature, it can be seen that no individual method of design is completely satisfactory for the design of slope in open pit mining. In fact, the choice of design method is often less important than the choice of the input parameters.

It is worth noting that for most problem geometries, Bishop's routine method has proven to give as accurate results as more rigorous slice methods. In fact, LEM with circular slip surfaces can be used in many situations for prediction of stability, without any great loss of accuracy [1].

Therefore, in this paper, the Bishop's Method based on the Method of Slices for slope stability analysis and the Hoek–Brown failure criterion is used due to its simple and popular application in geoen지니어ing practice.

4. Open pit mine planning process

Open pit mine planning and design is a decision-making process that leads to a realistic and actionable plan to profitably extract mineral resources. Planning can be carried out for a wide range of durations from the very short (next shift) to the very long (life of mine) [29]. This section of the paper briefly describes the long-term mine planning.

The mine planning practice in open pit begins with a block model that contains ore and waste. Together with the block model, it is necessary to prepare the input parameters. These parameters include slope angles, costs, prices and the metallurgical recovery.

Some of the costs are market based, for example, the costs of oil, shipping, equipment and construction services [29]. These costs are strongly influenced by the daily production of the mine and by the type of equipment being used [30].

Commodity price is the most difficult input variable to predict, yet it is the most important input variables impacting mine planning decisions as it has a direct influence on the optimal rate of production, the final pit size and the desired degree of operational flexibility that is built into the operation [29].

With the introduction of the input parameters, the optimisation process is carried out and the final pit is obtained. The final pit limit defines what is economically mineable from a given deposit; it identifies which blocks should be mined and which ones should be left in the ground [31].

Together with the determination of the final pit, a necessary step is to develop the mining sequence. This could be done by producing a nest of pits corresponding to various cut-off grades, which is accomplished by varying the price of the metal being extracted [32].

After obtaining the final pit and nested pits, mine designs are made through mine planning, which is usually an iterative process between the geotechnical engineer and the mine planner [33]. Mine designs break the overall pit reserve into manageable planning units called phases, which are commonly based on the sequence determined by the nested pit, although the following considerations must be taken into account [32]:

- The probable maximum ore and waste mining rate required in a given phase.
- The size and type of equipment to be used. This determines the required minimum operating bench width.
- Appropriate working, inter-ramp and final slope angles.

Based on these considerations, the mine planner proceeds to the design of phases ensuring that ramp access to each active bench is provided.

After mine designs are completed, the determination of the annual mining schedules based on mill feed or product requirements is made. It may be necessary to repeat the process of mine design of phases before an adequate plan is developed [32]. Schematically, the mine planning process is shown in Figure 9.

5. Case study

The case study chapter is divided into the following sub-sections: block model and cost parameters, geotechnical domains, geometrical components of a slope and the open pit mine planning process.

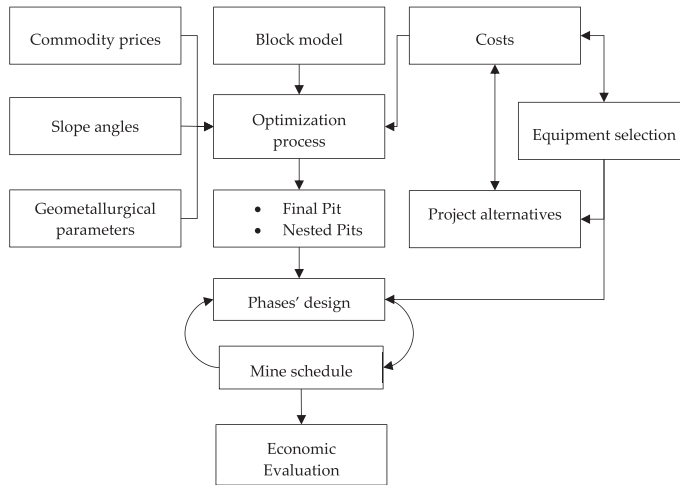


Figure 9. Mine planning stages.

Table 3. Economic parameters and metallurgical recovery.

Copper price (US\$/lb)	3
Mine cost (US\$/mt)	3.4
Processing cost (US\$/mt)	6.1
Metallurgical recovery (%)	85
Smelter and refining costs (US\$/lb)	0.85

5.1. Block model and cost parameters

The block model used in this work corresponds to a real deposit that contains copper ore. Due to a confidentiality agreement, the name and location of this deposit cannot be disclosed.

The characteristics regarding the dimensions of the model are as follows:

- Regular blocks of 10 m × 10 m × 10 m
- East–West length: 1625 m
- North–South length: 1630 m
- Depth: 360 m

The economic parameters and the metallurgical recovery values used are listed in Table 3.

From the values in Table 3, the marginal cut-off grade was calculated using Equation (8).

$$\text{ton}_i \cdot \frac{\text{rec}_i}{100} \cdot \frac{g_i}{100} \cdot (P - C_s) \cdot 2204.62 \left[\frac{\text{lb}}{\text{mt}} \right] = \text{ton}_i \cdot C_p \quad (8)$$

where ton_i = tonnage for block i [mt]; rec_i = metallurgical recovery for block i [%]; g_i = marginal cut – off grade for block i [%]; P = copper price $\left[\frac{\text{US\$}}{\text{lb}} \right]$; C_s = selling cost $\left[\frac{\text{US\$}}{\text{lb}} \right]$; C_p = processing cost $\left[\frac{\text{US\$}}{\text{mt}} \right]$.

Using values from Table 3 in Equation (8), the marginal cut-off grade was calculated to be 0.151%.

To understand the ore deposit, Figure 10 shows the distribution of the ore with grades above the marginal cut-off grade, which tend to be located in specific zones of the ore deposit.

For the scheduling stage, an annual movement of 5 million tonnes of ore from the mine to the processing plant and a total movement of 10 million tonnes of material was considered. Capital

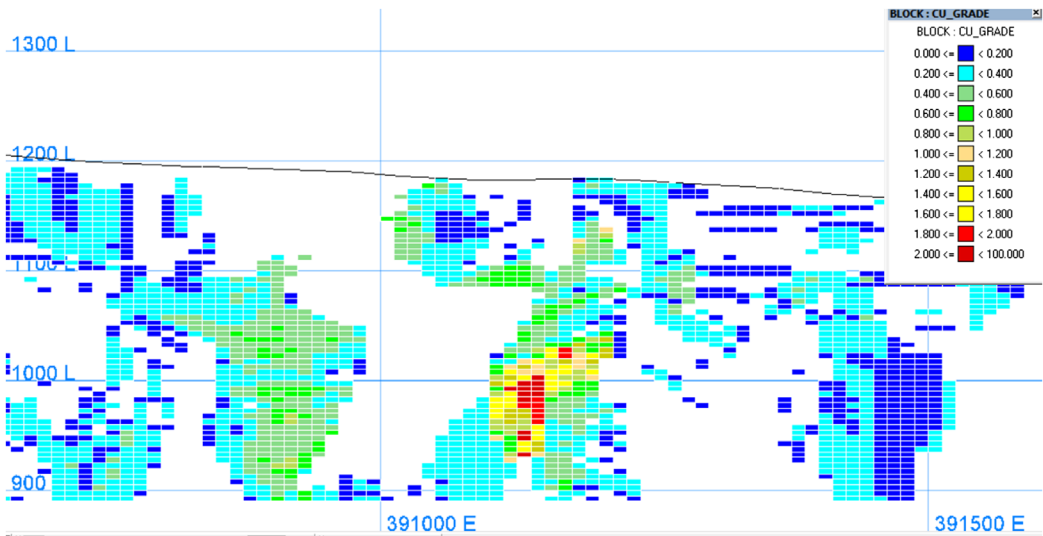


Figure 10. Representative profile view of an east-west section.

Table 4. Rock mass properties for each geotechnical domain.

	UCS (MPa)	GSI	Mi
Domain 1	65	45	15
Domain 2	50	45	12

investment of mining equipment was not considered as it was assumed that all mining was done using contractor’s equipment, the cost of which has already been incorporated in the mining cost. For the processing plant, an investment of US\$164 million was assumed.

5.2. Geotechnical domains

Two geotechnical domains were considered as presented in Table 4. The disturbance factor D was considered equal to 1 according to the geometric zone defined by Hoek and Karzulovic [12].

Figure 11 shows a representative plan view for the geotechnical domains in the block model. For clarity, only blocks above the marginal cut-off grade are displayed.

5.3. Geometrical components of a slope

Three scenarios of acceptance criterion were considered as shown in Table 5.

It was assumed that the stability was controlled by rock mass strength at all scales (bench, inter-ramp, global). A limit equilibrium analysis in two dimensions was carried out to determine the stability of the slopes.

A general guide in designing the benches is that the bench height should be matched to the loading equipment. For example, for small gold deposits, a typical value of the bench height is 7.5 m while a common bench height in today’s large open pits is 15 m [34]. In this study, a bench height of 10 m was used, which is consistent with the material movement described in sub-section 5.1 of this work. In addition, a double bench was considered whenever it was possible. For the berm width, the Ritchie’s formula was applied as follows [1]:

$$\text{bench width [m]} = (0.2 \cdot \text{bench height} + 4.5)[\text{m}] \tag{9}$$

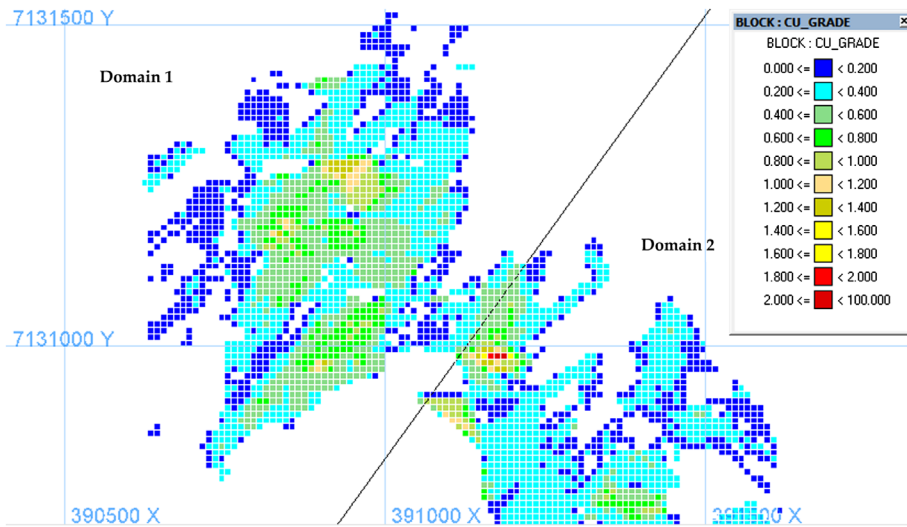


Figure 11. Plan view for level 1040.

Note: The line corresponds to a division between the two defined domains.

Table 5. Different scenarios of acceptance criteria.

Scenario	Global FoS	Inter-ramp FoS
Conservative	1.4	1.3
Neutral	1.3	1.2
Aggressive	1.2	1.1

The resulting value for the berm width when replacing the bench height in Equation (9) was 6.5 m. When considering a double bench configuration, i.e. a bench height of 20 m, then the resulting bench width was 8.5 m.

According to the geotechnical domains defined, for a double bench of 87° for domain 1, the resultant FoS at a bench scale was 1.46, which is higher than the admissible FoS for all scenarios. With this face bench angle (which is practically vertical), it is possible to obtain the inter-ramp heights for the different scenarios according to the admissible FoS at inter-ramp scale as described in Table 5.

To determine the global angle in accordance with the admissible FoS defined in Table 5, it was assumed that the maximum overall depth was 310 m, which was the maximum depth of the block model from the surface to the bottom of the block model. Because the depth of the pit shell is not known, in the first step of the optimisation, the overall depth must be assumed to be equal to the maximum block model depth from the surface to the bottom of the block model. After the first pit shell is obtained, a pit height (or depth) can be measured. Using Limit Equilibrium Method Analysis, a global slope angle according to an admissible FoS is obtained. With this slope angle, a second optimisation step is undertaken to obtain another pit shell. This iterative process must be performed until the global angle and pit depth have an admissible FoS (Figure 12). The results of the optimisation process for domain 1 are shown in Table 6.

The width criteria for the travelled lane of a straight haul segment should be based on the widest vehicle in use. For the two-way traffic, which is most common in open pit mines, the rule of thumb is that the roadway width should be at least three times the truck width [33]; Couzens recommends at least four times [34]. In this case study, a ramp width of 30 m was used, which is consistent with the hauling equipment for the material movement as described in sub-Section 5.1 of this work. If three ramps are assumed to be present within the slope, i.e. an inter-ramp height of approximately 100 m

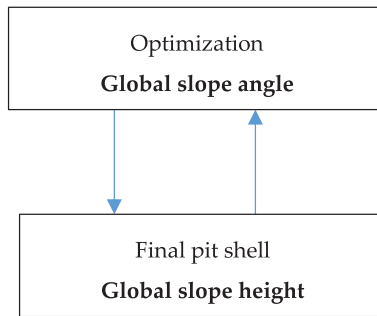


Figure 12. Iterative process to obtain the pit shell with a global slope angle adjusted to the admissible FoS.

Table 6. Overall FoS and slope angle.

Scenario	Domain 1		
	Aggressive	Neutral	Conservative
Admissible global FoS	1.2	1.3	1.4
Global slope height (m)	310	310	310
Global slope angle (°)	50.8	47.2	43.5
Global FoS	1.20	1.30	1.40

for every case, and considering a berm width of 8.5 m (Equation (9)) then the global angle obtained is higher than the one calculated using the admissible FoS for each scenario. In this specific case, the bench face angle must be decreased until it is consistent with the global slope angle calculated with the admissible FoS for each scenario. For Domain 2, the same methodology was carried out as the one described for Domain 1.

5.4. Open pit planning process

After the determination of the geometrical components of the slope and the final pit shell, the designs of the mining phases were undertaken. Ramps were designed with a grade of 10%. This value was supported by the literature review, which showed that a number of pits operate at 10% [34].

For the evaluation of production schedules, a discount rate of 10% was used. After obtaining the schedules, an evaluation in terms of the net present value (NPV) was carried out, and the Equilibrium Method analysis was performed for every three periods of each schedule to analyse the stability of the slopes of the mine designs.

6. Analysis of results

The analysis of results is divided in four parts: pit optimisations and phases' definition, pit designs, scheduling and economical evaluation and stability analysis by period.

6.1. Pit optimisation and phases' definition

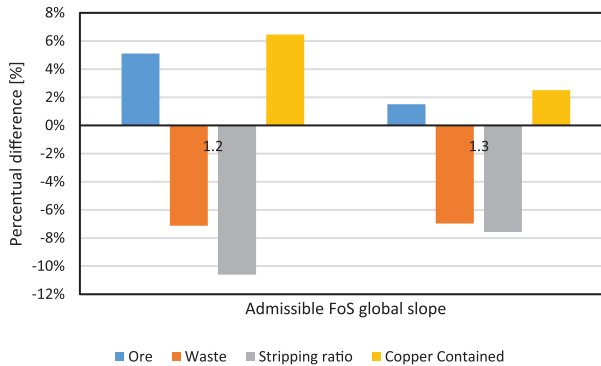
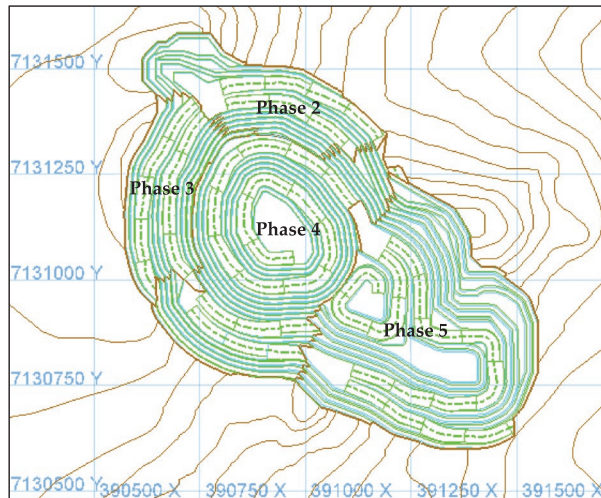
For the final pit shells, the results shown in Table 7 were obtained.

Figure 13 shows the differences between the scenarios in terms of ore, waste, stripping ratio and copper contained with respect to the scenario of an admissible FoS of 1.4 based on the values shown in Table 7.

As can be seen from Figure 13, the greater the admissible FoS, the greater the stripping ratio but the lower the copper contained.

Table 7. Tonnages, copper grades, stripping ratios and copper contained for the different scenarios.

Admissible FoS	Total tonnage (kT)	Ore tonnage (kT)	Waste tonnage (kT)	Copper grade (%)	Stripping ratio	Copper contained (Mlb)
1.2	184,106	116,046	68,060	0.43	0.59	1104
1.3	180,254	112,083	68,171	0.43	0.61	1063
1.4	183,694	110,415	73,279	0.43	0.66	1037

**Figure 13.** Differences in ore, waste, stripping ratio and copper contained between different scenarios with respect to the scenario of an admissible FoS of 1.4.**Figure 14.** Final pit design for an admissible FoS of 1.3.

6.2. Pit designs

As a result of the optimisation stage, the pit was divided into five phases. For all the scenarios considered, the phases were very similar in terms of the geometry. Figure 14 shows the final pit shape for an admissible FoS of 1.3.

The walls of phase 1 were fully mined by phases 2 and 3. This is the reason why phase 1 is not shown in Figure 14. The differences in percentages of ore, waste, stripping ratio and copper contained with respect to an admissible FoS of 1.4 are shown in Figure 15.

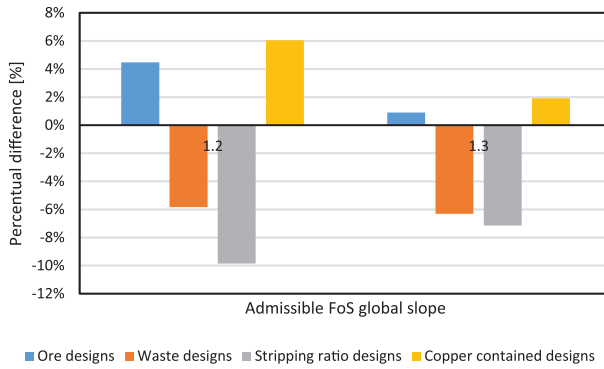


Figure 15. Differences in ore, waste, stripping ratio and copper contained between different scenarios with respect to the scenario of an admissible FoS of 1.4.

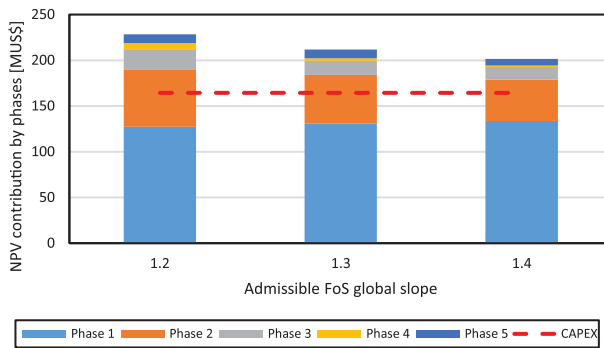


Figure 16. NPV contribution by phases.

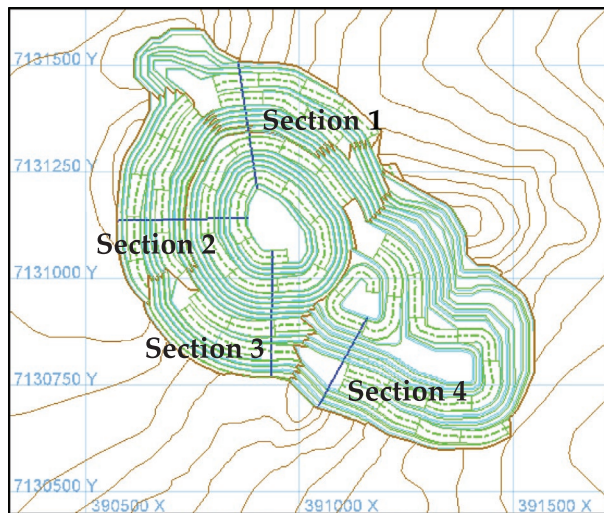


Figure 17. Sections for measuring the FoS in the final pit for the scenario of an admissible FoS of 1.3.

As can be seen from Figure 15, the tendency of the variables analysed in the final pit designs were very similar to the ones obtained in the optimisation stage for the final pit shells shown in Figure 13. It is, thus, possible to conclude that the results obtained are consistent in the optimisation and design stages.

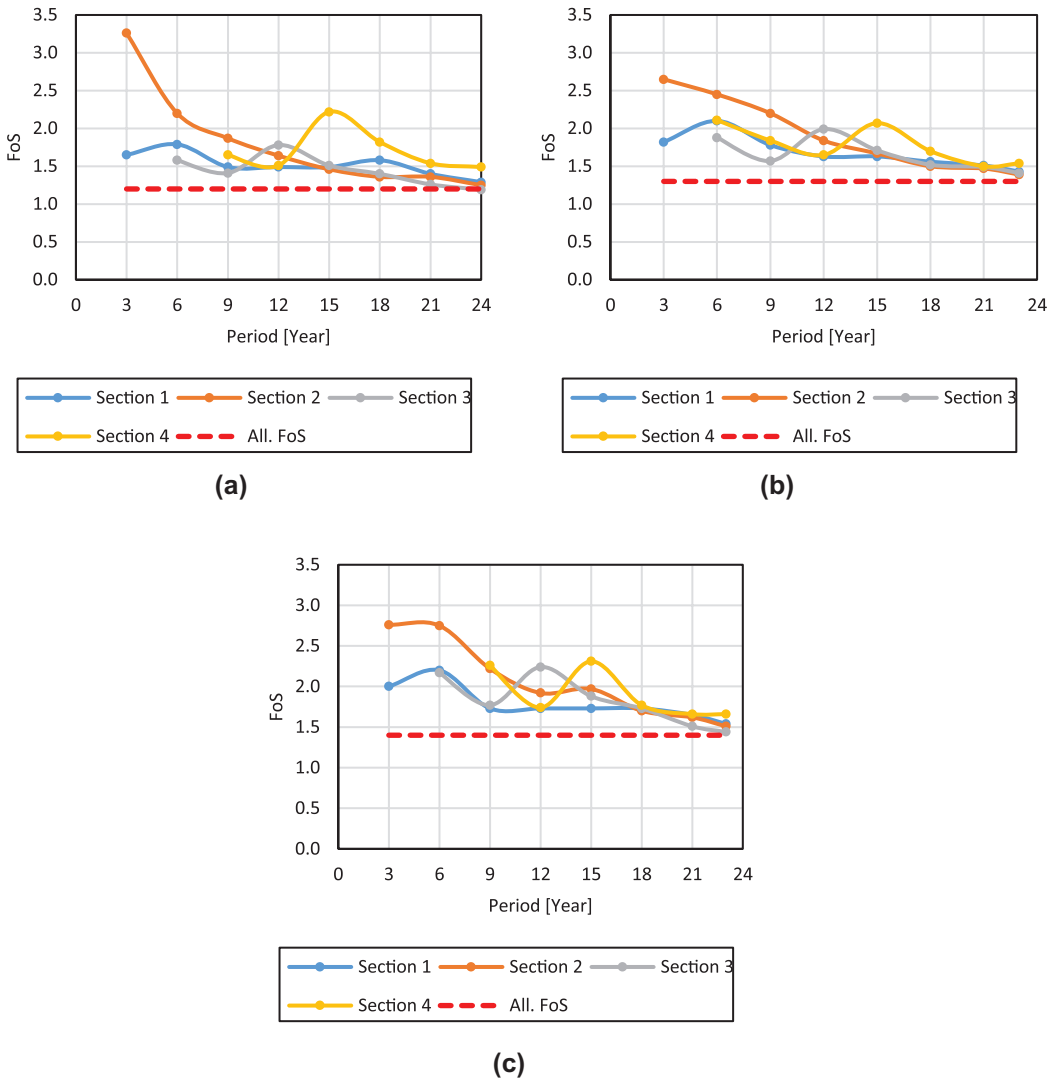


Figure 18. (a) FoS for the scenario corresponding to an admissible FoS of 1.2. (b) FoS for the scenario corresponding to an admissible FoS of 1.3. (c) FoS for the scenario corresponding to an admissible FoS of 1.4.

6.3. Scheduling and economical evaluation

The contribution to the NPV by phases according to the different scenarios of admissible FoS are shown in Figure 16.

As can be seen from Figure 16, phase 1 is the one that gives the greatest contribution to the NPV due to its high benefit related with a higher copper grade and its low stripping ratio. The other reason is that phase 1 is extracted first, which means it has less discount rate than the other phases.

6.4. Stability analysis by period

In Figure 17, the final pit for an admissible FoS of 1.3 with the sections for analysing the slope stability is shown. The measurement of the FoS in the profiles was conducted every 3 years of the mine schedule. The locations of the sections for the cases corresponding to admissible FoS of 1.2 and 1.4 are very similar to the ones shown in Figure 17.

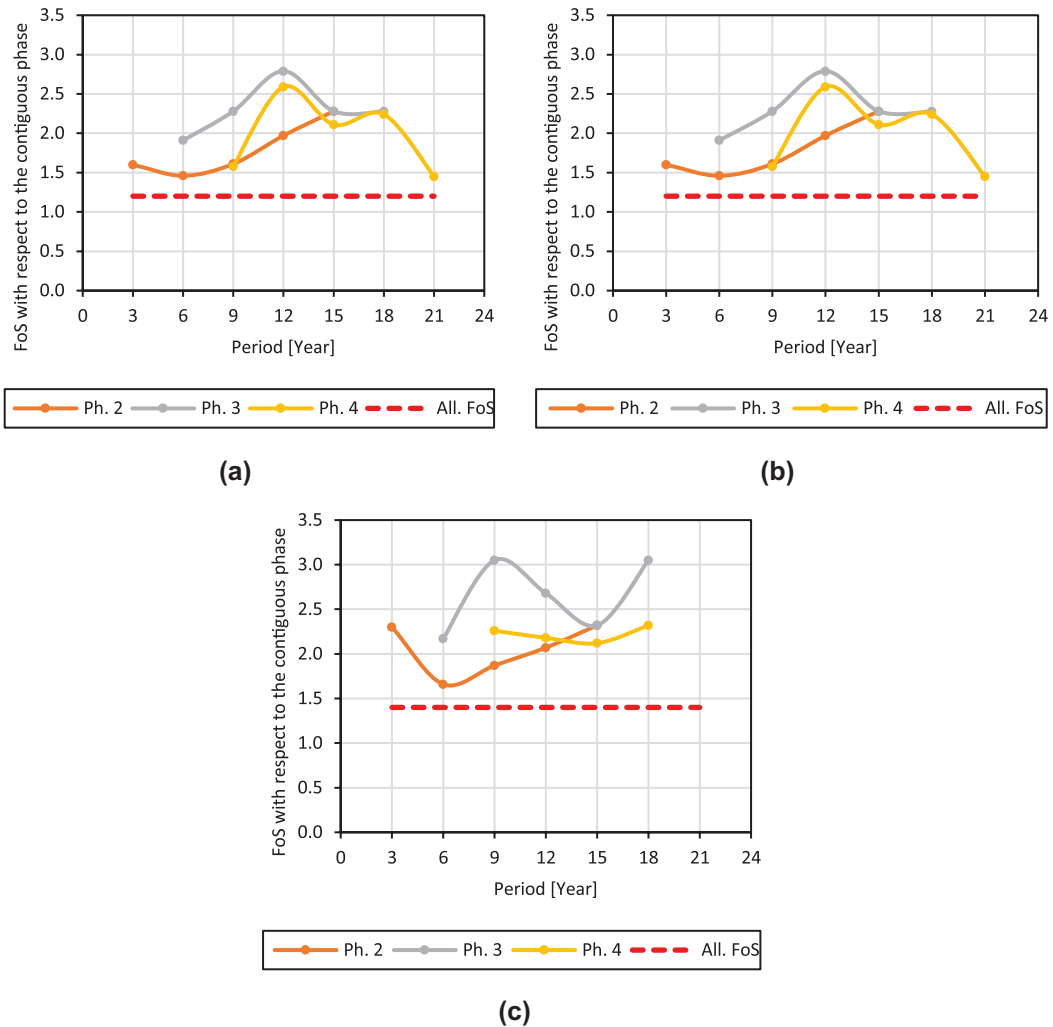


Figure 19. (a) FoS for adjacent phases corresponding to the scenario of an admissible FoS of 1.2. (b) FoS for adjacent phases corresponding to the scenario of an admissible FoS of 1.3. (c) FoS for adjacent phases corresponding to the scenario of an admissible FoS of 1.4.

As shown in Figure 18, the FoS of the slopes have a decreasing tendency as the pit goes deeper, converging to the admissible FoS. Nevertheless, there are certain periods in which the FoS of the sections increases as occurs in year 12 for Section 3 and in year 15 for Section 4. This occurs because the incorporation of ramps in those sections makes the slope angle decrease considerably during those periods.

As can be seen in Figure 19, the FoS between adjacent phases is considerably greater than the admissible FoS at a global scale. If an admissible FoS at an inter-ramp scale is considered, this difference is even greater. As a result, it would be possible to increase the slope angles that do not belong to the final pit wall between contiguous phases.

7. Conclusions

This study of integration of the FoS into the mine planning was carried out using Bishop’s Method based on Method of Slices and Hoek–Brown failure criterion to determine the geometric components of a slope for different scenarios of FoS.

In general, different admissible FoS for the determination of slopes angles of an open pit, impact the entire mine planning process and affect the final economic value of a project. The most important outcome of the analysis presented in this paper shows that, in pit walls that do not correspond to the final pit, it would be possible to increase the slope angles. The impact of increasing the value of temporary slope angles would certainly imply an increment in the NPV of a project. For this reason the possibility of increasing those slope angles should be included in the methodology of every project.

Additionally, the following conclusions may be drawn:

- The NPV increases as the admissible FoS decreases, as expected.
- The main difference that occurred in each scenario of the case study was in the stripping ratio where the greater the admissible FoS, the greater the stripping ratio because, as the admissible FoS increases, the amount of ore decreases. The reverse situation tends to occur with waste.
- In the pit walls that belong to the final pit, the FoS in the mine schedule converges to the admissible FoS.

In future studies, other factors should be taken into account, such as, rock mass properties, presence of water and discontinuities, among others, which may influence the slope stability to various degrees. In addition, probabilistic aspect of rock characteristics affecting slope stability, which are not part of the scope of the present work, should be studied.

Acknowledgements

The authors would like to thank the following persons and organisations for their support in this work: CONICYT BASAL Grant FB0809 through the Advanced Mining Technology Center for supporting this work. Dr. Eleonora Widzyk-Capehart for her assistance in editing the manuscript.

Disclosure statement

No potential conflict of interest was reported by the authors.

Funding

This work was supported by the Advanced Mining Technology Centre, CONICYT BASAL Grant [FB0809].

ORCID

Phu Minh Vuong Nguyen  <http://orcid.org/0000-0002-4895-8811>

References

- [1] J. Sjöberg, *Analysis of large scale rock slopes*, Ph.D. thesis, Lulea University of Technology, Lulea, 1999.
- [2] A.R. Bye and F.G. Bell, *Stability assessment and slope design at Sandsloot open pit, South Africa*, Int. J. Rock Mech. Min. Sci. 38 (2001), pp. 449–466.
- [3] Pictured: The largest North American landslide EVER that dropped 165 MILLION tons more than half a mile down at copper mine in Utah, 2013. Available at <http://www.dailymail.co.uk>.
- [4] J. Franz, *An investigation of combined failure mechanisms in large scale open pit slopes*, Ph.D. thesis, School of Mining Engineering, The University of New South Wales, Sydney, Australia, 2009.
- [5] J. Wesseloo and J. Read, *Acceptance Criteria, in Open Pit Slope Design*, CSIRO, Leiden, 2013, pp. 221–236.
- [6] C. Edelbro, *Rock mass strength – A review*, Tech. Rep. Department of Civil Engineering, Division of Rack Mechanics, Lulea University of Technology, Lulea, 2003.
- [7] E. Hoek and E.T. Brown, *Underground Excavations in Rock*, Institution of Mining and Metallurgy, London, 1980.
- [8] E. Hoek, *Strength of jointed rock masses*, Géotechnique. 33 (1983), pp. 187–223.
- [9] E. Hoek and E.T. Brown, *The Hoek–Brown Failure Criterion*, Proceedings of the 15th Canadian Rock Mechanics Symposium, University of Toronto, Toronto, 1988, pp. 31–38.

- [10] E. Hoek, P.K. Kaiser, and W.F. Bawden, *Support of Underground Excavations in Hard Rock*, A.A. Balkema, Rotterdam, 1995.
- [11] E. Hoek and E.T. Brown, *Practical estimates of rock mass strength*, Int. J. Rock Mech. Min. 34 (1997), pp. 1165–1186.
- [12] E. Hoek and A. Karzulovic, *Rock Mass Properties for Surface Mines*, in *Slope Stability in Surface Mining*, Society for Mining, Metallurgy and Exploration, Littleton, CO, 2001.
- [13] E. Hoek, C. Carranza-Torres, and B. Corkum, *Hoek–Brown Failure Criterion – 2002 edition*, Proceeding of the 5th North America Rock Mechanics Symposium and 17th Tunnelling Association of Canada Conference, University of Toronto, Toronto, 2002, pp. 267–271.
- [14] E. Hoek, D. Wood, and S. Shah, *A Modified Hoek–Brown Failure Criterion for Jointed Rock Masses*, Proceeding of the international ISRM Symposium on Rock Characterisation – EURock, British Geotechnical Society, Chester, 1992, pp. 209–214.
- [15] E. Hoek, *A Brief History of the Hoek–Brown Criterion*, Program, RocLab, 2002.
- [16] E. Hoek and J. Bray, *Rock Slope Engineering*, 3rd ed., IMM, London, 1981.
- [17] Z.T. Bieniawski, *Rock Mass Classification in Rock Engineering*, in *Exploration for Rock Engineering*, Vol. 1, Balkema, Cape Town, 1976, pp. 97–106.
- [18] Z.T. Bieniawski, *The Geomechanics Classification in Rock Engineering Applications*. in *Proceedings of 4th Congress of International Society of Rock Mechanics*, Montreux, Vol. 2, Balkema, Rotterdam, 1979, pp. 41–48.
- [19] Z.T. Bieniawski, *Engineering Rock Mass Classifications*, Wiley, New York, 1989.
- [20] D.H. Laubscher, *Geomechanics classification of jointed rock masses – mining applications*, Trans. Refs. 477 of Inst. Min. Metall. Sect. A: Min. Ind. 86 (1977), pp. A1–A8.
- [21] A. Haines and P.J. Terbrugge, *Preliminary Estimate of Rock Slope Stability Using Rock Mass Classification Systems*. 7th Congress of International Society of Rock Mechanics, Aachen, Germany, 1991, pp. 887–892.
- [22] L. Lorig, P. Stacey, and J. Read, *Slope Design Methods*, in *Open Pit Slope Design*, CSIRO, Leiden, 2013, pp. 237–264.
- [23] L.W. Abramson, T.S. Lee, S. Sharma, and G.M. Boyce, *Slope Stability and Stabilization Methods*, Wiley, New York, 1996.
- [24] J.M. Duncan and S.G. Wright, *The accuracy of equilibrium methods of slope stability analysis*, Eng. Geol. 16 (1980), pp. 5–17.
- [25] A. Vyazmensky, *Numerical modeling of surface subsidence associated with block caving mining using a finite element/discrete element approach*, Ph.D. thesis, Simon Fraser University, 2008.
- [26] Rocscience, *Phase2 – 2D Elasto-plastic Finite Element Stress Analysis Program for Underground or Surface Excavations in Rock or Soil*, Rocscience, Toronto, 2005.
- [27] Itasca, UDEC and FLAC 3D, Itasca Consulting Group, Minneapolis, MN, 2004. Available at <http://www.itascacsg.com>.
- [28] Rockfield, ELFEN. Rockfield Software, UK, 2001. Available at <http://www.rockfield.co.uk/elfen>.
- [29] D. Whittle, *Open-pit Planning and Design*, in *SME Mining Engineering Handbook*, Society for Mining, Metallurgy, and Exploration, Englewood, CO, 2011, pp. 877–901.
- [30] E. Bozorgebrahimi, R.A. Hall, and G.H. Blackwell, *Sizing equipment for open pit mining – a review of critical parameters*, Min. Technol. (2003), pp. 171–179.
- [31] K. Dagdelen, *Open Pit Optimization – Strategies for Improving Economics of Mining Projects Through Mine Planning*, International Mining Congress and Exhibition of Turkey, Leiden, 2001.
- [32] W. Hustrulid, M. Kuchta, and R. Martin, *Production Planning*, in *Open Pit Mine Planning and Design*, CRC, Leiden, 2013, pp. 504–669.
- [33] P. Williams, J. Floyd, G. Chitombo, and T. Maton, *Design Implementation*, in *Open Pit Slope Design*, CSIRO, Leiden, 2013, pp. 265–326.
- [34] W. Hustrulid, M. Kuchta, and R. Martin, *Geometrical considerations*, in *Open Pit Mine Planning and Design*, CRC, Leiden, 2013, pp. 290–408.